

Modeling of Groundwater Yield Using GIS and Electrical Resistivity Method in a Basement Complex Terrain, Southwestern Nigeria

**Ilugbo Stephen Olubusola^{1*}, Adebisi Ayodele Daniel¹
and Olomo Kazeem Oladimeji¹**

¹*Department of Applied Geophysics, Federal University of Technology, Akure, Ondo State, Nigeria.*

Authors' contributions

This work was carried out in collaboration between all authors. Author ISO designed the study, performed the statistical analysis, wrote the protocol and first draft of the manuscript. Authors AAD and OKO managed the analyses of the study. Author ISO managed the literature searches. All authors read and approved the final manuscript.

Article Information

DOI: 10.9734/JGEESI/2018/42102

Editor(s):

(1) Masum A. Patwary, Geography and Environmental Science, Begum Rokeya University, Bangladesh.

Reviewers:

(1) Sunday Olufemi Adesogan, University of Ibadan, Nigeria.

(2) Nordiana Mohd Muztaza, Universiti Sains Malaysia (USM), Malaysia.

Complete Peer review History: <http://www.sciencedomain.org/review-history/25087>

Original Research Article

**Received 27th March 2018
Accepted 6th June 2018
Published 11th June 2018**

ABSTRACT

In this research, groundwater yield of Ibodi and its environs have been investigated using hydrogeologic data and vertical electrical sounding. The study was carried out with a view to providing information on the geoelectric characteristic of the subsurface sequence, bedrock topography, subsurface structural features and their hydrogeologic significance, in order to determine possible areas for groundwater yield zones. The study involved the use of Schlumberger vertical electrical sounding data at sixty-eight (68) stations. The results from depth sounding data interpretation revealed four subsurface geoelectric layers namely; the topsoil, weathered layer, fractured basement and the fresh basement. The weathered layer and fractured basement constitutes the aquifer units with varying thickness. The second order parameters were determined from the interpretation of vertical electrical sounding results and used to determine the groundwater yield index value (G.W.Y.I) by multiplying the coefficient of anisotropy (λ) and total transverse resistance (T) i.e. ($\lambda * T$). The groundwater yield index value was used to model the groundwater

*Corresponding author: E-mail: bussytex4peace44@gmail.com;

yield map The groundwater yield of the entire study area was classified into very high, high yield, moderate yield, low yield and Very low yield. The boreholes data and static water level across the entire study area were used to validate the accuracy of the groundwater yield map and hence of the proposed methodology. The locations and names descriptions of these boreholes and static water level were displayed on the groundwater yield map. The validation was carried out by superimposing the boreholes and static water level data on the groundwater yield map.

Keywords: Coefficient of anisotropy; groundwater yield; GIS; geoelectric sections.

1. INTRODUCTION

Groundwater is one of the most valuable natural resources on the earth surface and serves as one of the main sources of drinking water. Basement complex have problem of potable groundwater supply due to the crystalline nature of the underlying rock which lack primary porosity [1,2]. Groundwater storage capacity in those areas is dependent on depth of weathering and intensity of fracturing of the underlying rock. For basement complex rock to become good aquifers, they must be highly fractured and highly weathered [3]. Thickness of the weathered overburden and fractured zone determined the nature and intensity of hydrodynamic activities within the usually discrete bodies of aquifer in the terrain [3,4,2,5]. Therefore, the assessment and development of groundwater at both local and regional level requires multidisciplinary approaches, with various data sources by mapping these localized geological structures [5]. Apart from the application methods for exploring groundwater, the availability of groundwater depends on various geological factors such as rock types, existence of lineaments and structures suitable for accumulating the resources, hydrological and hydrogeological factors. All these are dependent on the type of geological terrains in consideration for the exploration [6,2]. In typical basement complex areas such as the study area, the occurrence of groundwater in recoverable quantity as well as its circulation is controlled by geological factors *i.e.* faults, joints and fracture zones [7,4,2]. The delineation of these features is very essential for better understanding of the subsurface geology of these areas in term of their groundwater potential. Therefore to target potential basement aquifers that can give copious supply of groundwater in these areas, the aforementioned geologic features must be intercepted by boreholes. Therefore to target potential basement aquifers that can give copious supply of groundwater in these areas, the aforementioned geologic features must be intercepted by boreholes. Thus, groundwater

potential of a basement complex area is determined by a complex interrelationship between the geology, post-emplacements, tectonic history, weathering processes and depth, composition of the weathered layer, aquifer types and combination, groundwater flow pattern, climate, recharge and discharge processes [8] cited in [2]. The groundwater potential of such area is therefore dependent on the following factors; the presence of large fractures, joints or brecciated zones within the rock, the extent of weathered overburden and degree or amount of precipitation recharging the aquifer. By far most significant factor in the groundwater capacities of an area underlain by crystalline rock is the depth of weathering. The absolute depth of weathering has implications on the zone of saturation because groundwater is known to fill the regolith from phreatic surface down to the basement [2]. The Dar-Zarrouk parameters are obtained from the first order parameters (geoelectric parameters) which are Total longitudinal unit conductance (S), Total transverse unit resistance (T), and coefficient of anisotropy (λ). Electrical anisotropy is a measure of the degree of in homogeneity [9,10] in a basement terrain; which arises from near-surface effects, variable degree of weathering and structural features such as faults, fractures, joints, foliations, and beddings. These in turn are responsible for creating secondary porosity (Φ_s) and hence effective porosity (Φ_e). Since the basement rocks are significantly anisotropic and the degree of electrical anisotropy can be measured in terms of the anisotropy coefficient (λ). Also the groundwater yield, Y, is a function of the volume of the accumulated groundwater and the permeability of an aquifer. This is influenced, controlled, and dependent on the effective porosity (Φ_e). The degree of inhomogeneity, expressed as electrical coefficient of anisotropy (λ), correlates linearly with groundwater yield; Hence, $Y = f(\lambda)$. Consequently, the geoelectric parameters that would be of hydrologic significance to evaluate the groundwater yield of a given area will be largely determined by the prevailing factors that influence the occurrence of

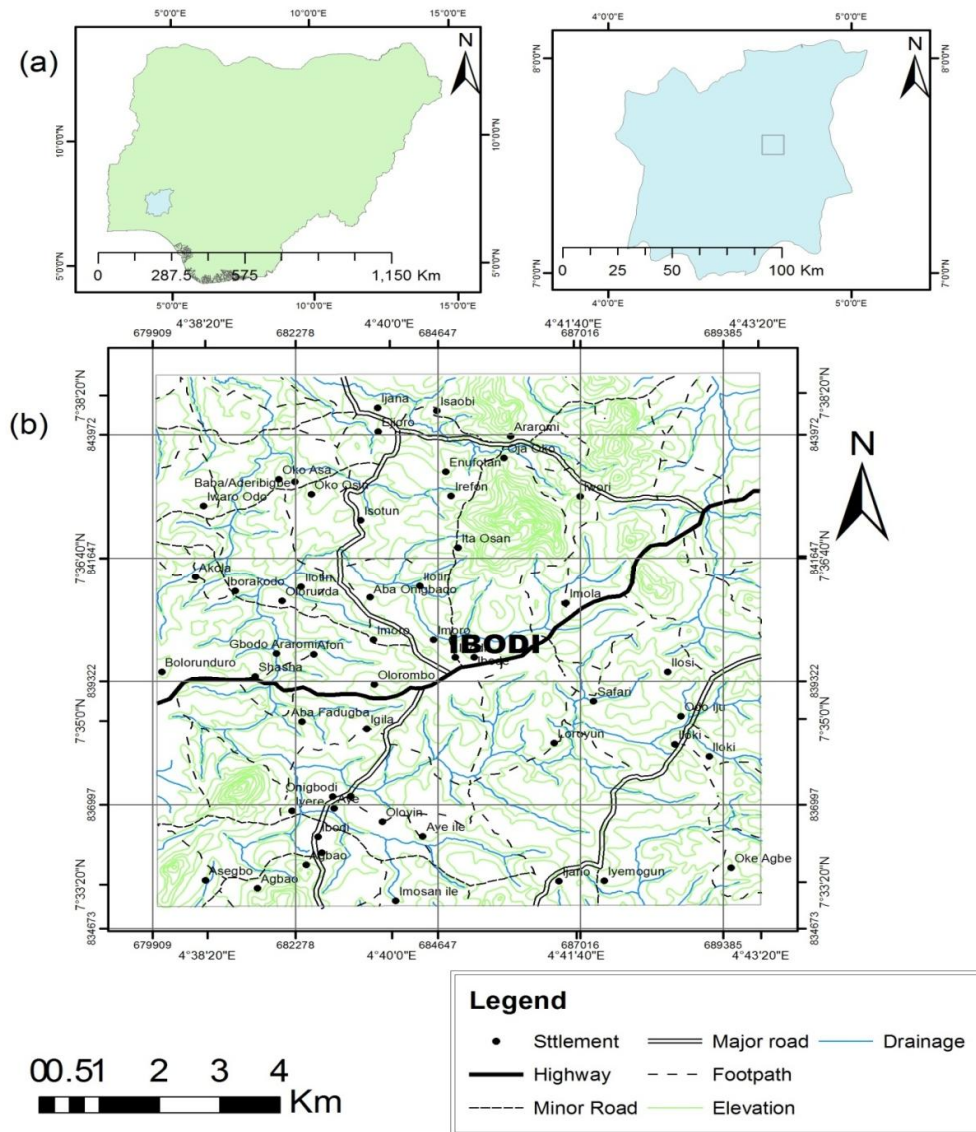


Fig. 1(a). Map of Nigeria and Osun State showing the study area, (b) Location map of Ibodi and its environ showing the study area [11]

the resources in the area. In other words, prediction of groundwater yield capacity is a spatial decision problem that typically involves a large set of feasible alternatives. Therefore, in this research work Electrical resistivity methods were used around Ibodi and its environs in order to evaluate the groundwater yield.

1.1 Study Location and Geology

The investigated area comprises of sixty-eight (68) villages which are located on the crystalline

basement complex. It falls within latitude $7^{\circ} 32' 20''$ to $7^{\circ} 38' 20''$ North and longitude $4^{\circ} 36' 20''$ to $4^{\circ} 44' 20''$ East (Fig. 1). This area falls within the 1:50,000 topographical map of Ilesha sheet 234 SW. Major and minor road linkages characterize the study area linking both towns and villages in the area. In general, the study area can be said to be fairly assessible with footpaths in areas where there are neither major nor minor roads. Regionally, the study area belong to the Southwestern Nigeria basement complex comprising migmatite-gneiss complex,

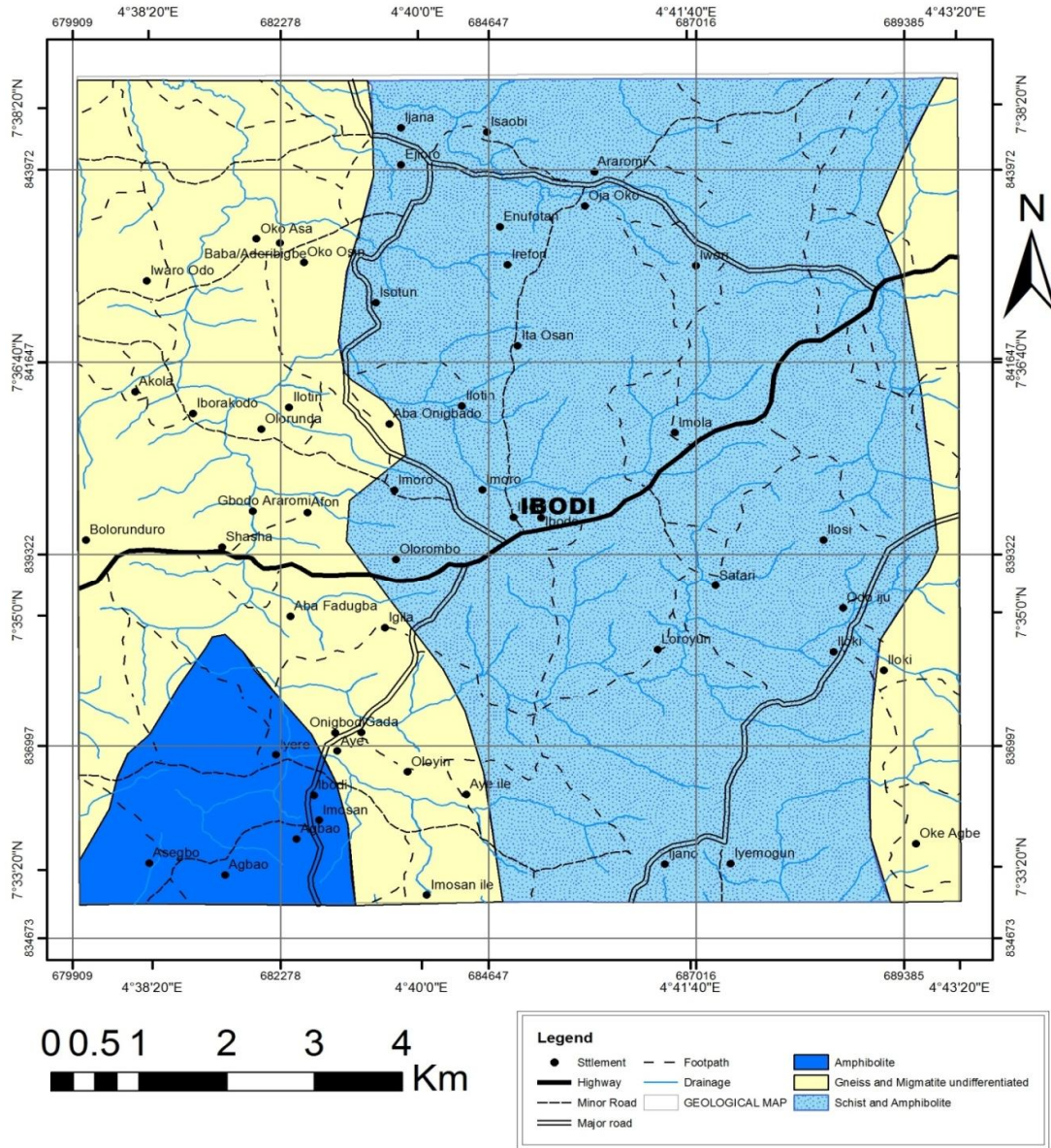


Fig. 2. Geological map of Ibodi and its environs [14]

metagneous rock such as pelitic schist, quartzite, amphibolites, charnockitic rocks, older granite and unmetamorphosed dolerite dykes. The rock sequence consists of basically weathered quartzite of older granite. The basement complex rocks of Nigeria are made up of heterogeneous assemblages [12,13]. The geology of Ibodi and its environs is mainly Precambrian Basement rock (Fig. 2). This is because of the tectonics and metamorphic changes that has occurred in the area [15]. Schist and amphibolites, magnetite -

gneiss undifferentiated and amphibolites stands out in the Basement rock of the investigated area.

2. RESEARCH METHODOLOGY

Sixty eight (68) vertical electrical sounding were obtained within the investigated area (Fig. 3). The sounding data were presented as sounding curves, which are plots of apparent resistivity values against electrode separation (AB/2) and (AB/3) on bi-log graph. The Schlumberger depths

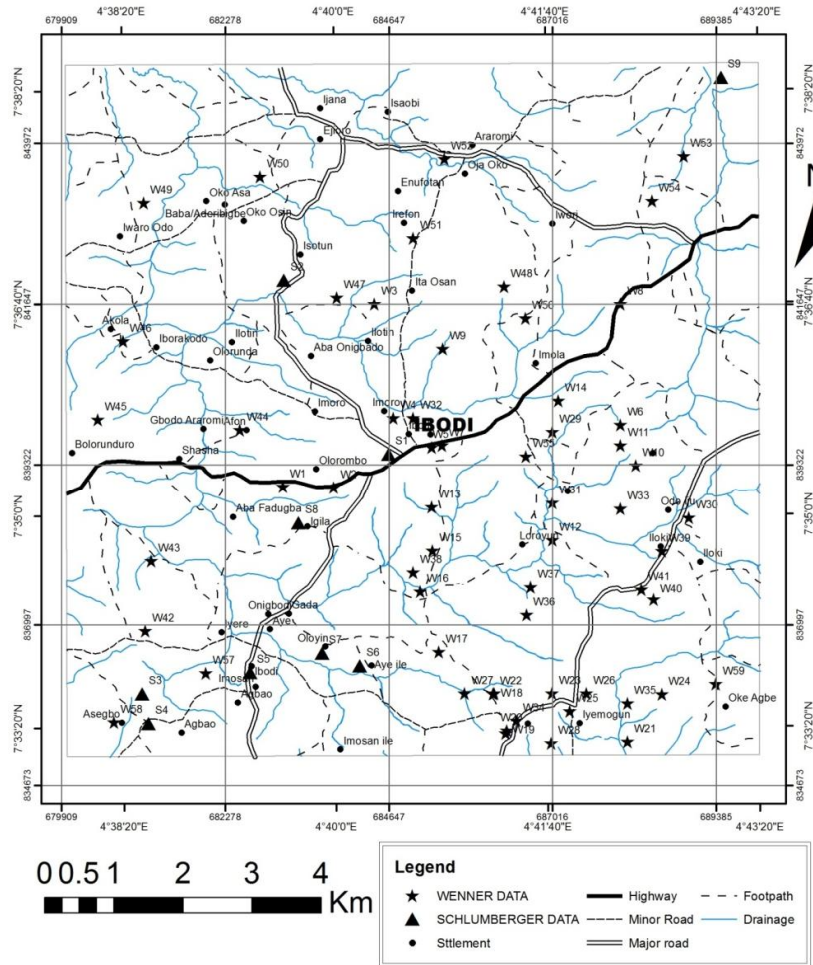


Fig. 3. Data acquisition map of the study area showing the VES data

sounding are used to investigate the change of resistivity with depth [16,17]. The measured unit is the apparent resistivity, ρ_a , which is the product of a geometrical factor, K, and the quotient of the measured potential, ΔV , and the source current, I. The apparent resistivity is plotted versus AB/2 or AB/3 in meters on bilogarithmic paper resulting in a VES curve. The VES curve showed the change of resistivity with depth, since the effective penetration increases with increasing electrode spacing. The interpretation of the VES curve is both qualitative and quantitative. The qualitative interpretation involved visual inspection of the sounding curves while the quantitative interpretation utilized partial curve matching technique using 2-layer master curve which was later refined by a computer iteration technique Resist version (Vander, 2004) that is based upon an algorithm of [18]. The quantitatively interpreted sounding curves gave interpreted results as geoelectric parameters

(that is, layer resistivity and layer thickness). The Dar-Zarrouk parameters are obtained from the first order parameters (geoelectric parameters) which are Total longitudinal unit conductance (S), Total transverse unit resistance (T), and coefficient of anisotropy (λ) using this mathematical expressions. Electrical anisotropy is a measure of the degree of in homogeneity [9], [10] in a basement terrain; which arises from near surface effects, variable degree of weathering and structural features such as faults, fractures, joints, foliations, and beddings. These in turn are responsible for creating secondary porosity (Φ_s) and hence effective porosity (Φ_e). Since the basement rocks are significantly anisotropic and the degree of electrical anisotropy can be measured in terms of the anisotropy coefficient (λ). Also the groundwater yield, Y, is a function of the volume of the accumulated groundwater and the permeability of an aquifer. This is influenced, controlled, and

dependent on the effective porosity (Φ_e). However, in this present study, these parameters have been developed further through the application of the product of the coefficient of anisotropy (λ) and the total transverse resistance (T) i.e. ($\lambda \cdot T$) to determine the groundwater yield index value which was found to be very relevant and useful in determination and evaluation of groundwater yield. The groundwater yield index value was used to model the groundwater yield map and the borehole and static water level data across the entire study area were used to validate the groundwater yield.

to have a detailed description of the lateral and vertical variation in resistivity, thickness and topography of the subsurface rocks, the VES interpretation results were used to prepare three (3) geoelectric sections across the study area, that align approximately along SW-NE, N-E and NW-SE direction as shown in the Fig. 5a to 5c. The geoelectric sections of the study area show a total of three to five subsurface layers namely: the topsoil, weathered layer, fractured basement and fresh basement.

3. RESULTS AND DISCUSSION

3.1 Sounding Curves and Aquifer Types

Data acquired from vertical electrical sounding (VES) using Schlumberger and Wenner depth sounding were interpreted, first using manual partial curve matching techniques, and later subjected to computer iterative modeling. In the study area, eight (8) curve types were identified, these are A, H, QH, HA, KH, KHA, KQH, KHK (Fig. 4a to 4h). Where type curve KH has the highest percentage (32.4%) of occurrence. The least percentage of (1.5%) corresponds to the KHA.

3.3 Geoelectric Section along SW – NE Direction

The first layer constitutes the topsoil with layer resistivity ranging from 95 Ωm to 1228 Ωm (Fig. 5a). The layer thickness varies from 0.7 to 1.6m. The varying resistivity suggests topsoil of clay, clayey sand, sandy clay and sand. The second layer with the resistivity ranging from 38 Ωm to 568 Ωm is the weathered layer. The layer thickness varies from 0.7m to 49.7m. This layer can also be referred to as aquifer layer especially in areas like Ibodi (VES 1), Agbao (VES 3), Imoro (VES 41), Iwori (VES 63), Imola (VES 65) and VES 11 where the weathered layer is not clayey. The third layer constitutes the fractured basement which can also be referred to as aquifer layer, they are interpreted as saturated because of their relatively lower resistivity values i.e. ranging from 222 Ωm to 854 Ωm . The thickness of this layer varies from 4.5 m to 54.9 m beneath VES3, VES 8 and VES 9. The thickness

3.2 Geoelectric Section

In order to have better understanding of the nature of the rock underlying the study area, and

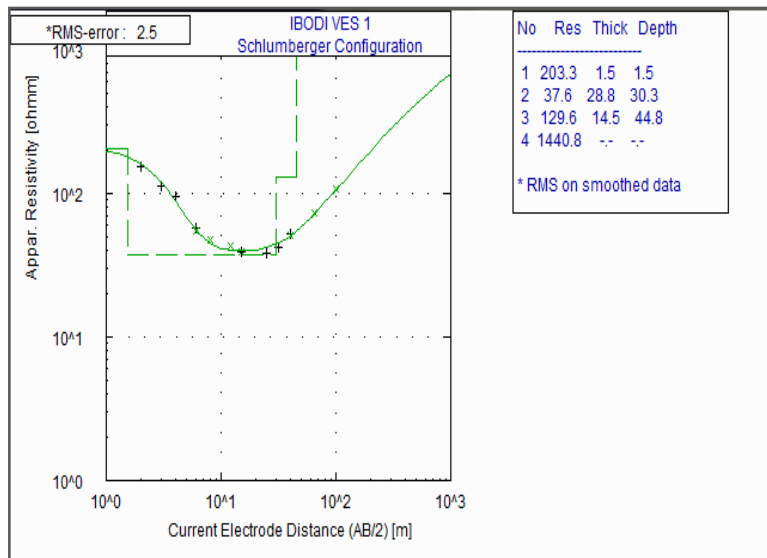


Fig. 4a. Showing typical curve types HA curve

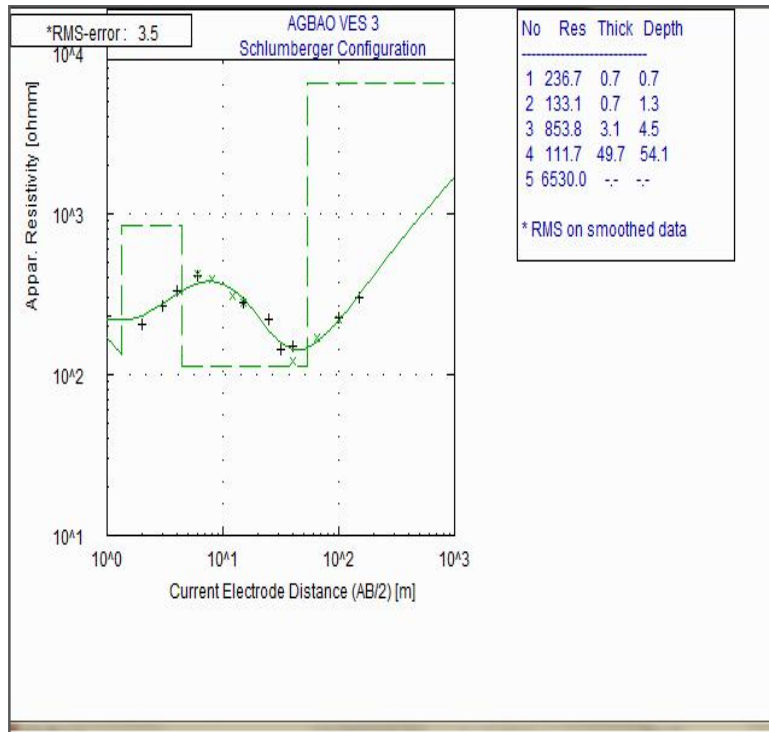


Fig. 4b. Showing typical curve types HKH curve

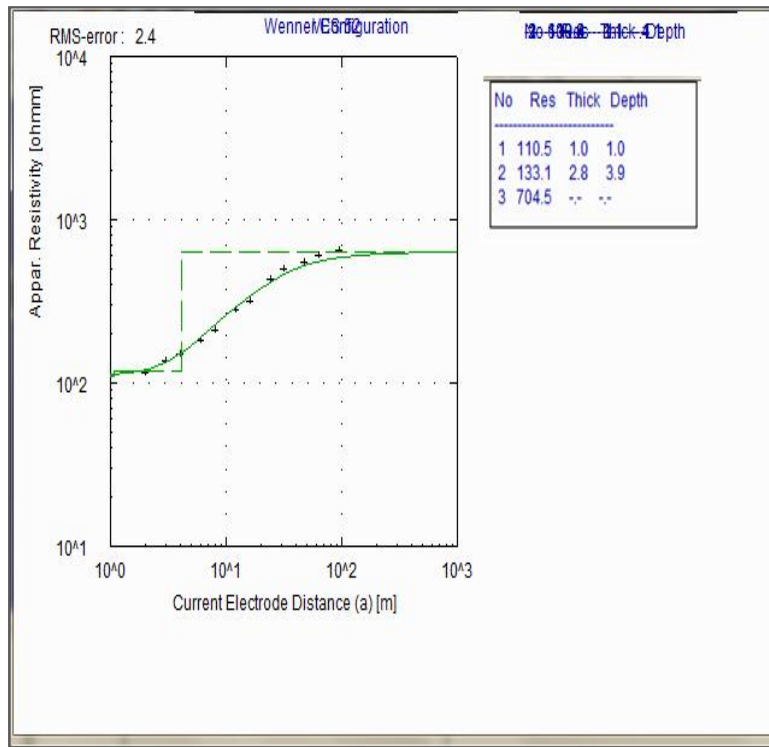


Fig. 4c. Showing typical curve types A curve

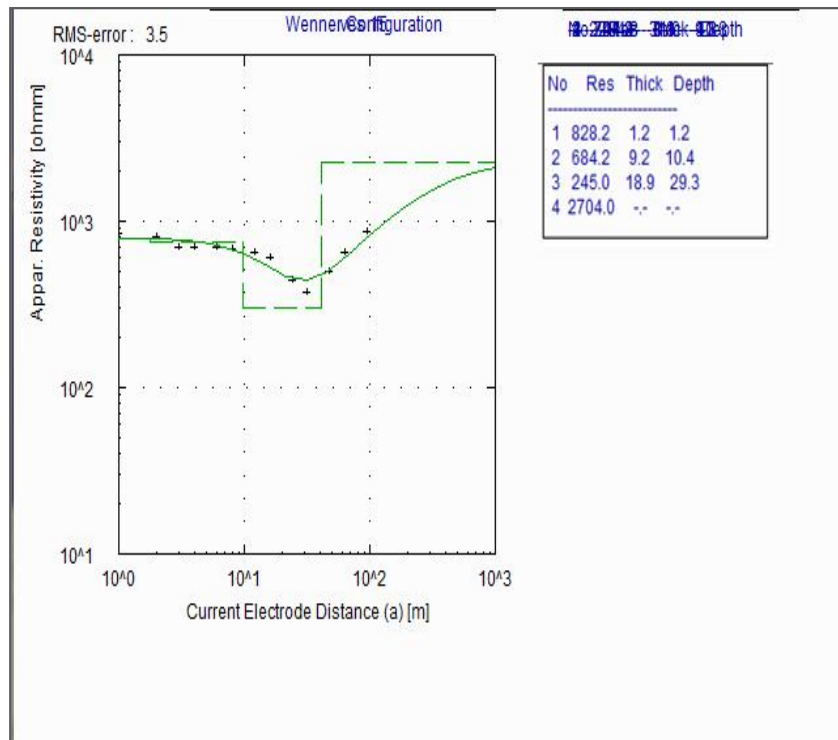


Fig. 4d. Showing typical curve types QH curve

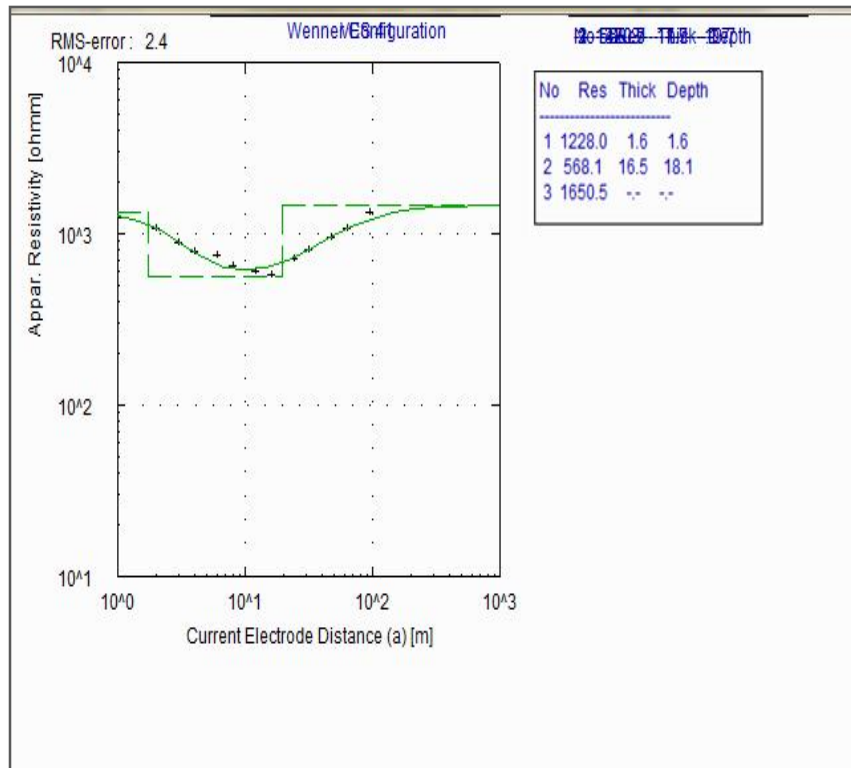


Fig. 4e. Showing typical curve types H curve

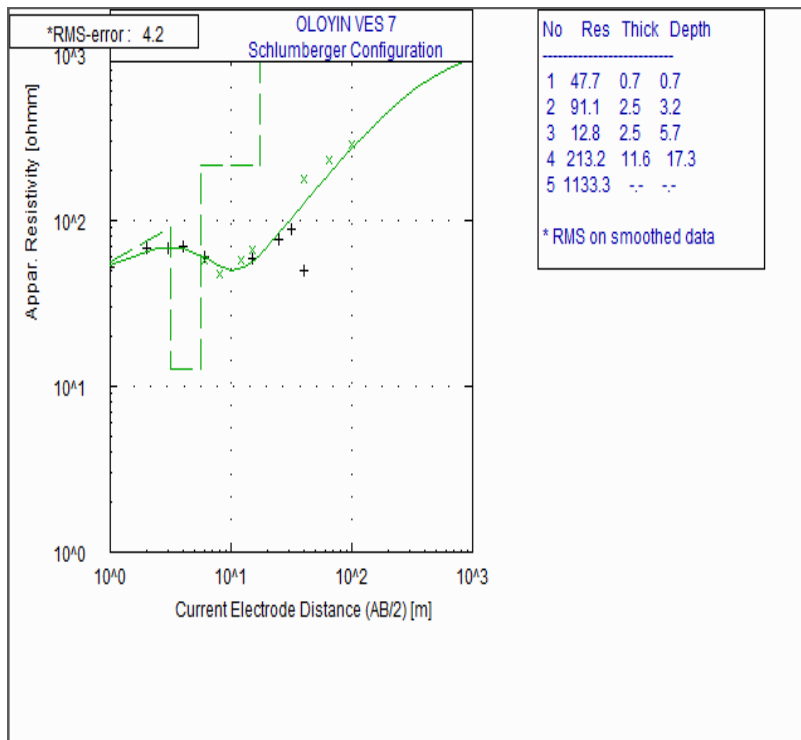


Fig. 4f. Showing typical curve types KHA curve

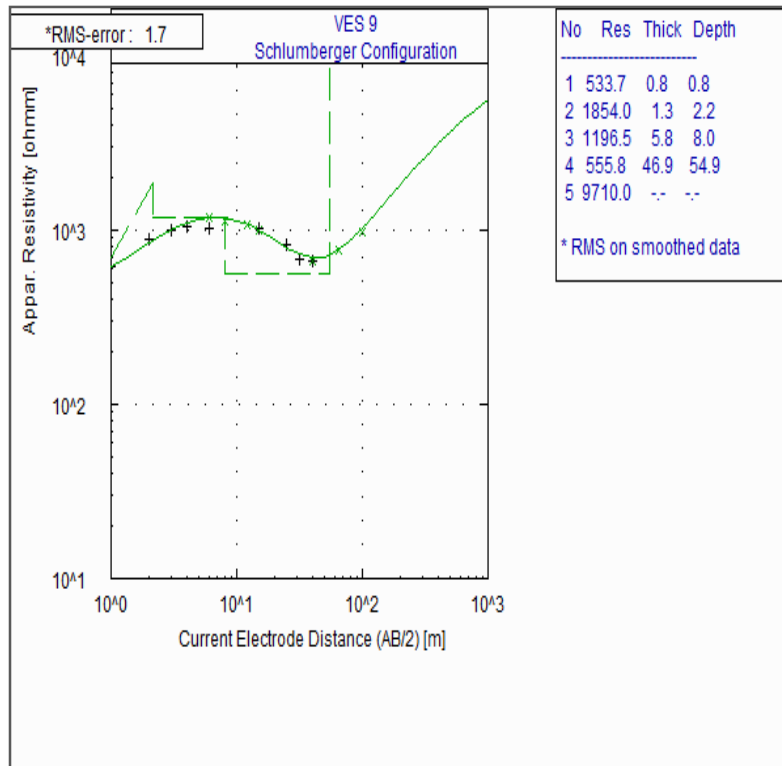


Fig. 4g. Showing typical curve types KQH curve

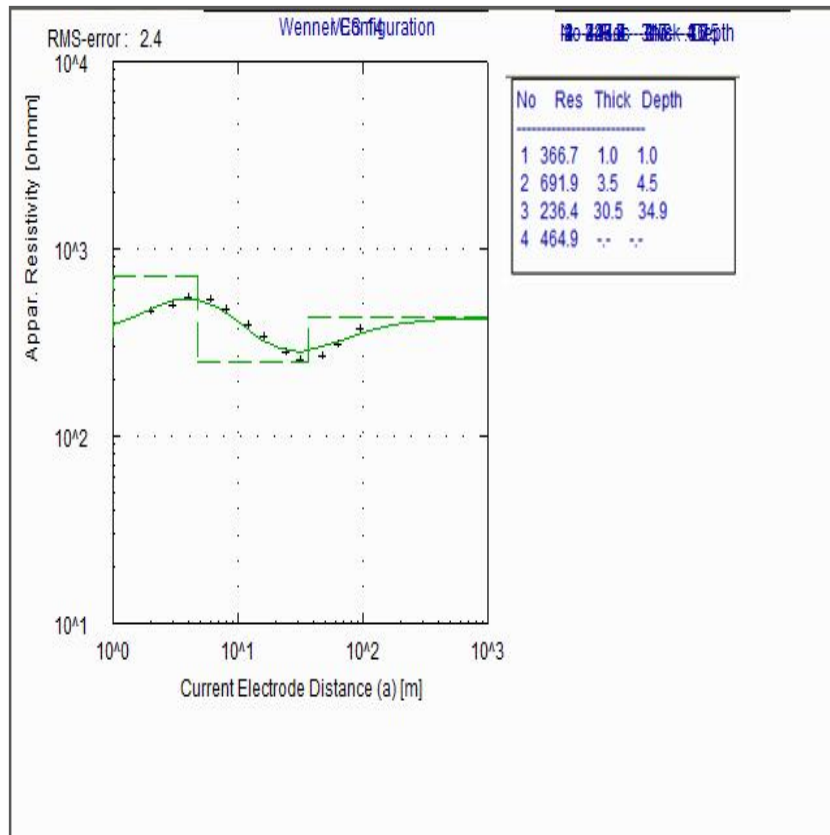


Fig. 4h. Showing typical curve types KH curve

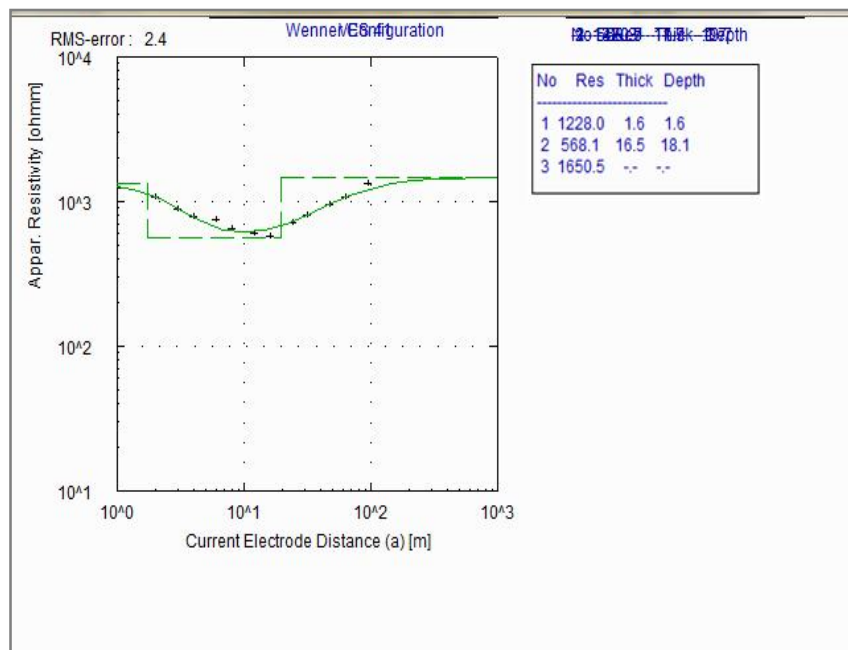


Fig. 4e. Showing typical curve types H curve

of that VES 8 tend to infinite. The fourth layer is the fresh basement which is characterized by high resistivity values ranges from 980 Ωm to 9710 Ωm . The fresh basement is made up of infinitely resistive rock. The rocks in this zone are hard with no permeability, and hence it is not a water-bearing zone. Depth to fresh rocks from the interpretation of sounding curves is found to range between 1.5 m to 54.1 m. The bedrock topography is undulating.

thickness of this layer varies from 7.4 m to 30.5 m. Beneath VES13, VES 14 and VES 68, the thickness tend to infinite. The fourth layer is the fresh basement which is characterized by high resistivity values ranges from 1230 Ωm to 4878 Ωm . The fresh basement is made up of infinitely resistive rock. The rocks in this zone are hard with no permeability, and hence it is not a water-bearing zone. The bedrock topography is undulating.

3.4 Geoelectric Section along NW – SE Direction

The first layer constitutes the topsoil with layer resistivity ranging from 141 Ωm to 1228 Ωm (Fig. 5b). The layer thickness varies from 0.9 to 2.0m. The varying resistivity suggests topsoil of clay, clayey sand, sandy clay and sand. The second layer with the resistivity ranging from 133 Ωm to 568 Ωm is the weathered layer. The layer thickness varies from 4.1 m to 29.5 m. This layer can also be referred to as aquifer layer especially in areas like Imoro (VES 41), Iborakodo (VES 49) and Iwaro Odo (VES 58). The third layer constitutes the fractured basement which can also be referred to as aquifer layer, they are interpreted as saturated because of their relative lower resistivity values i.e. ranging from 236 Ωm to 799 Ωm . The

3.5 Geoelectric Section along W – E Direction

The first layer which is the topsoil has resistivity varying from 103 Ωm to 1040 Ωm and thickness ranging from 0.7 m to 2.7 m (Fig. 5c). This layer is relatively thin and highly resistivity. The resistivity of the second layer which is the weathered zone varies from 70 Ωm to 945 Ωm while its thickness varies from 0.7m to 49.7 m. The third layer constitutes the fractured basement which is also be referred to as aquifer layer, they are interpreted as saturated of their relatively lower resistivity ranging from 226 Ωm to 859 Ωm . The thickness tends to infinite beneath VES 5, VES 31 and VES 68, while the fourth layer is the fresh basement with resistivity values ranging from 1607 Ωm to 6530 Ωm .

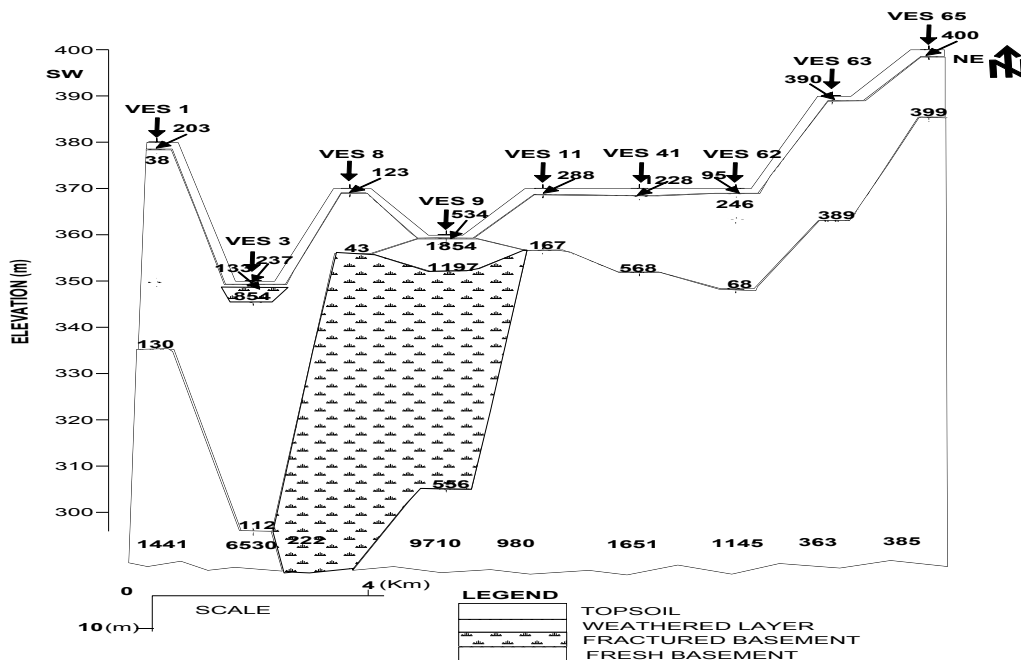


Fig. 5a. Geoelectric section along SW – NE direction

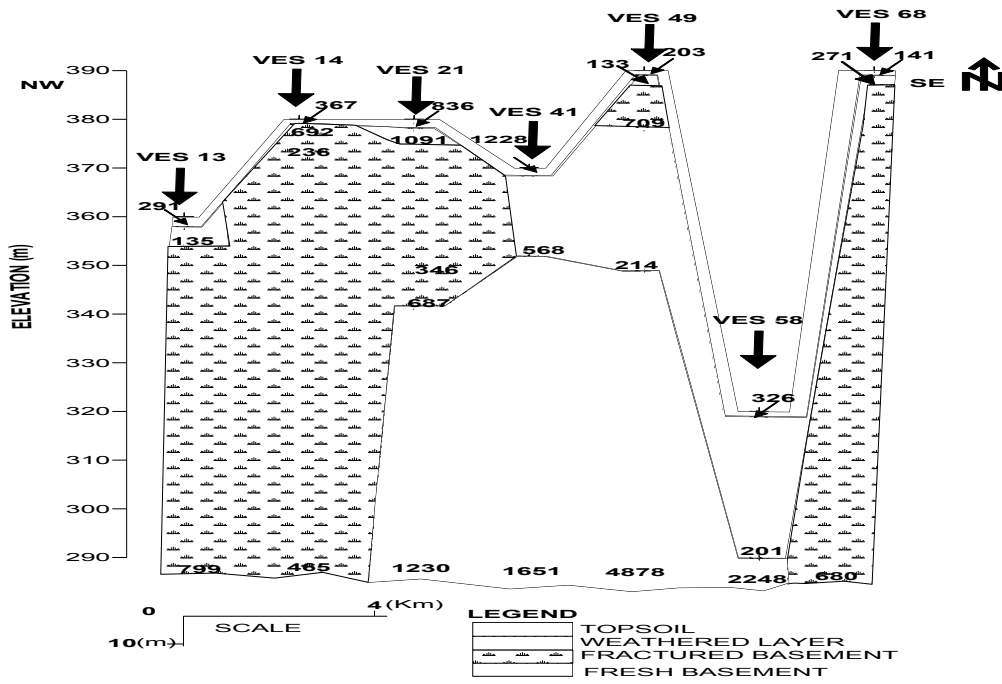


Fig. 5b. Geoelectric section along NW – SE direction

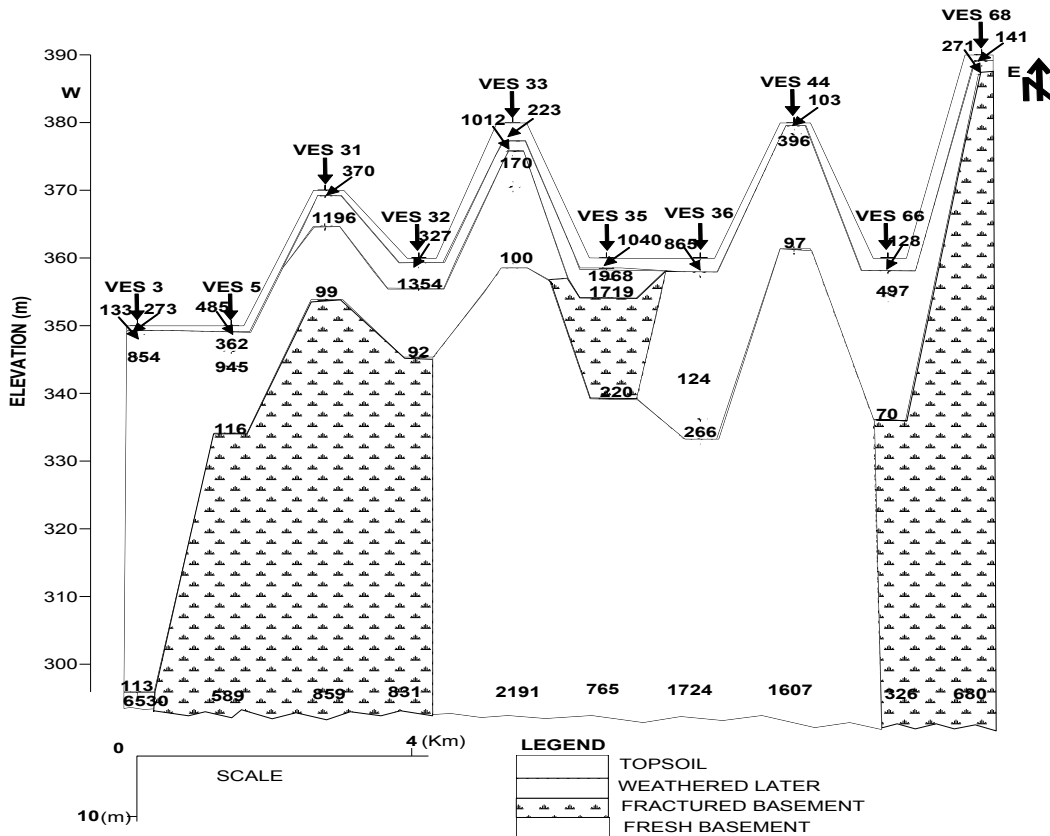


Fig. 5c. Geoelectric section along W – E direction

3.6 Dar Zarrouk Parameters for Groundwater Characteristics

The coefficient of anisotropy is estimated along with the secondary geoelectric parameters. The estimated value of coefficient of anisotropy is shown in Fig. 6. The estimation shows that the total longitudinal conductance varies from 0.0041 to 0.89 Ω^{-1} in the area. The qualitative use of this parameter is to demarcate changes in total thickness of low resistivity materials. The total transverse resistance ranges from 483.2 to 49,719.3 Ωm , which gives information both about the thickness and resistivity of the area. The average longitudinal resistivity calculated from sounding curves ranges 22.3 to 318.9 Ωm in the area, which helps in calculating the total depth H to the high resistivity bedrock and the average transverse resistivity varies from 17.6 to 807.2 Ωm , which clearly shows that it is more than the average longitudinal resistivity. This indicates that the true resistivity normal to the plane of structural features is greater than the true resistivity parallel to the plane of structural features. Based on these estimates it was found

that the coefficient of anisotropy ranges from 0.91 to 1.87, which depicts the true variation of the anisotropy character of rock formation. The area with high values of coefficient of anisotropy suggests that the fracture system must have extended in all the directions with different degrees of fracturing, which had greater water – holding capacity from different directions of the fracture(s) within the rock resulting in higher porosity. At the same time, unidirectional fracture may not produce good yield of water and such areas show low values of coefficient of anisotropy. Consequently, it indicates the presence of macro-anisotropy in the present geoelectric structures in the area. The coefficient of anisotropy shows that it increases from SE to SW and NE directions and reaches a maximum values close to 1.9 in the SW direction, as shown in anisotropy map (Fig. 6). It indicates that this physical property is not uniform in all directions and anisotropy plays a major role in fracturing. Here, it indicates more fracturing toward NE direction and thus suggests comparatively more groundwater potential zone and hence better prospect for groundwater availability.

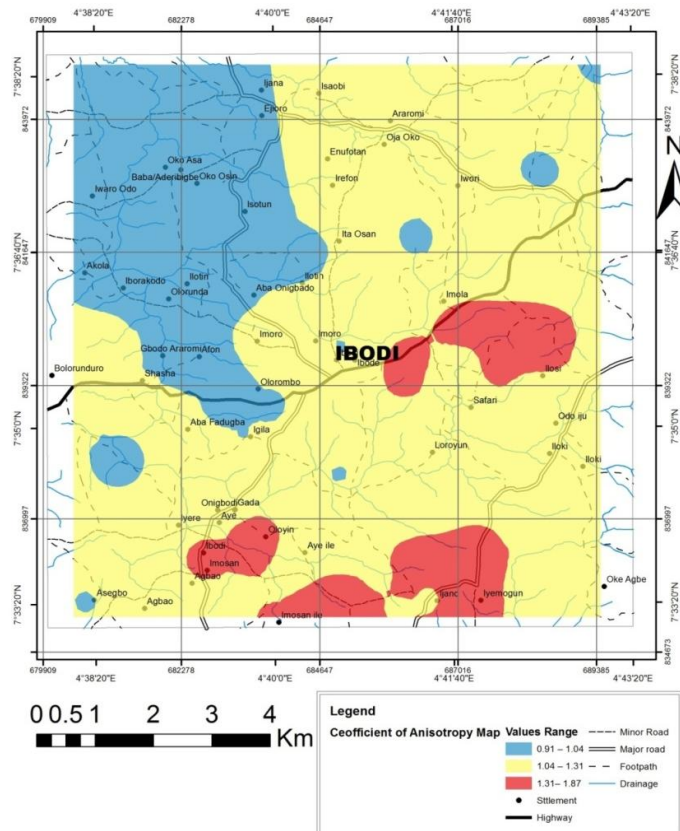


Fig. 6. Coefficient of anisotropy map of the study area

3.7 Modeling of Groundwater Yield Map

The Dar-zarrouk parameters are exclusively relevant in the lithological differentiation and delineation of aquifer geometry. In these applications, full advantage is taken of the combinations of thickness and resistivities into one single variable that is the coefficient of anisotropy which is used as bases for the evaluation of properties. However, in this present study, these parameters have been developed further through the application of the product of the coefficient of anisotropy (λ) and the total transverse resistance (T) i.e. ($\lambda \cdot T$) to determine the groundwater yield index value which was found to be very relevant and useful in determination and evaluation of groundwater yield. The groundwater yield index value was used to model the groundwater yield map which has a value ranging between 474 groundwater yield index to 137,703 groundwater yield capacity index, with the least rating being from 474 to 2000 G.W.Y.I. which implies very low yield, while between 2000 to 5000 G.W.Y.I., implies low yield and 5000 to 10000 G.W.Y.I., implies very moderate yield, while between 10000 to 30000 G.W.Y.I., implying

high yield, while 30000 G.W.Y.I. and above stands for very high yield (Fig. 7). Therefore, base on this, the entire study area was classified into very high, high yield, moderate yield, low yield and Very low yield. The extreme southern part and small closure that the southeastern has very high groundwater yield while eastern, southeastern and small closure at the northeastern and southwestern part has high groundwater yield and moderate groundwater yield dominate most of the area at northern, northeastern, eastern, southeastern, southern, south western and small closure at the northwestern part of the study area. The rest are dominated with low groundwater yield with small closure of very low groundwater yield at southwestern part. The boreholes data and static water level across the entire study area, were used to validate the accuracy of the groundwater yield map and hence of the proposed methodology. The locations and names descriptions of these boreholes and static water level were displayed on the groundwater yield map shown in Fig. 7. The validation was carried out by superimposing the boreholes and static water level data on the groundwater yield map.

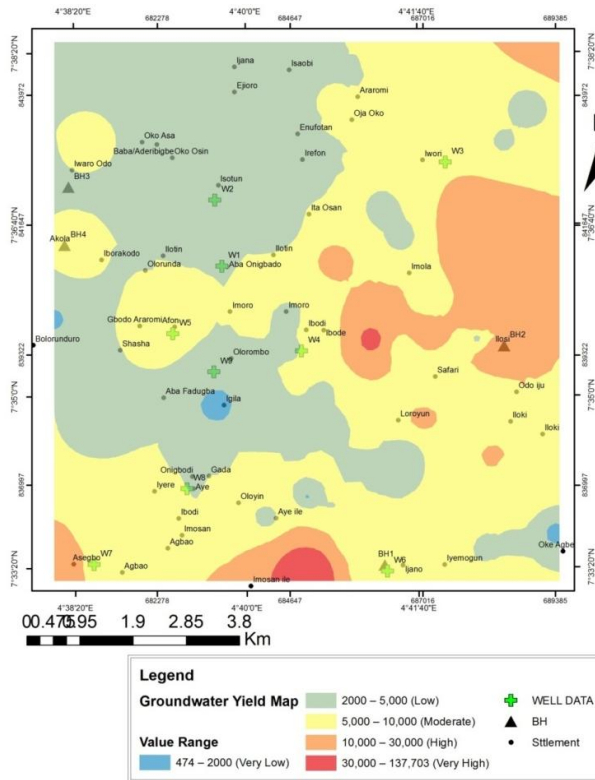


Fig. 7. Groundwater yield map of the study area

Table 1. Validation borehole for the groundwater yield map

Borehole number	Expected yield description from the groundwater yield map	Actual yield from the drilled borehole (litres/hr)	Actual description	Remarks
BH1	Low	662	Low	Coincide
BH2	High	3004	High	Coincide
BH3	Low	660	Low	Coincide
BH4	Moderate	817	Moderate	Coincide

Table 2. Validation of wells data for the groundwater yield map

Well numbers	Depth (m)	Static water level (m)	Groundwater yield thickness (m)	Expected yield description from the groundwater yield map	Actual yield from the wells (m)	Remarks
W1	12.9	12	0.9	Low	Low	Coincide
W2	8.6	8.3	0.3	Low	Low	Coincide
W3	11.8	11.15	0.65	Low	Low	Coincide
W4	6.8	6	0.8	Moderate	Low	Not Coincide
W5	13	12.9	0.1	Very low	Very low	Coincide
W6	13.3	13	0.3	Moderate	Low	Not Coincide
W7	10.6	9.7	0.9	Low	Low	Coincide
W8	8.2	7.1	1.1	Moderate	Moderate	Coincide
W9	18.6	dry	Dry	Very low	Very low	Coincide

3.8 Validation of Groundwater Yield Map

Pumping test results from boreholes drilled and static water level across the entire study area, were used to validate the accuracy of the groundwater yield map and hence of the proposed methodology. The locations, names and the actual yield descriptions of these boreholes and static water level are displayed on the groundwater yield map shown in Fig. 7. The validation was carried out by superimposing the boreholes on the groundwater yield map. The actual yield of each borehole was then compared with the expected yield of its location on the groundwater yield map. A Table showing coincidence (agreement) between the actual and the expected yields is presented in Table 1 and 2. Based on this table, the success rate of the prediction is estimated as follows:

Total number of boreholes = 4

Number of boreholes where the expected the actual yield classifications coincide = 3

Number of boreholes where the expected the actual yield classifications did not coincide = 1

Success rate (accuracy) of the groundwater potential map is = $\frac{3}{4} \times 100 = 75\%$

Total number of wells = 9

Number of wells where the expected the actual yield classification coincide = 7

Number of wells where the expected the actual yield classification did not coincide = 2

Success rate (accuracy) of the groundwater potential map is = $\frac{7}{9} \times 100 = 78\%$

Success rate (accuracy) of the groundwater potential for both borehole and wells data is = $\frac{11}{13} \times 100 = 85\%$

This approach shows that the proposed method in this study is capable of producing reliable and accurate results

4. CONCLUSIONS

In this research, groundwater yield of Ibodi and its environs have been investigated using hydrogeologic data and vertical electrical

sounding. The depth sounding data interpretation revealed four subsurface geoelectric layers namely; the topsoil, with thickness and resistivity ranging from 0.7 m – 2.7 m and 95 Ω m – 1228 Ω m respectively; the weathered layer, with thickness and resistivity ranging from 0.7 m – 49.7 m and 38 Ω m – 945 Ω m respectively; the fractured basement with resistivity ranging from 222 Ω m – 859 Ω m and thickness tending from 4.5 m – infinite; and the fresh basement with resistivity ranging from 980 Ω m – 9710 Ω m. The weathered layer and fractured basement constitutes the aquifer units with varying thickness. The second order parameters were determined from the interpretation of vertical electrical sounding results and used to determine the groundwater yield index value (G.W.Y.I) by multiplying the coefficient of anisotropy (λ) and total transverse resistance (T) i.e. (λ^*T). To determine the groundwater yield index value, this was found to be very relevant and useful in determination and evaluation of groundwater yield. The groundwater yield index value was used to model the groundwater yield map which has a value ranging between 474 groundwater yield index to 137,703 groundwater yield capacity index, with the least rating being from 474 to 2000 G.W.Y.I. which implies very low yield, while between 2000 to 5000 G.W.Y.I., implies low yield and 5000 to 10000 G.W.Y.I., implies very moderate yield, while between 10000 to 30000 G.W.Y.I., implying high yield, while 30000 G.W.Y.I. and above stands for very high yield. Therefore, base on this, the entire study area was classified into very high, high yield, moderate yield, low yield and Very low yield. The extreme southern part and small closure that the south eastern has very high groundwater yield while eastern, southeastern and small closure at the north eastern and south western part has high groundwater yield and moderate groundwater yield dominate most of the area at northern, northeastern, eastern, southeastern, southern, southwestern and small closure at the north western part of the study area. The rest are dominated by low groundwater yield with small closure of very low groundwater yield at southwestern part. The boreholes data and static water level across the entire study area, were used to validate the accuracy of the groundwater yield map and hence of the proposed methodology. The locations and names descriptions of these boreholes and static water level were displayed on the groundwater yield map. The validation was carried out by superimposing the boreholes and static water level data on the groundwater yield map.

COMPETING INTERESTS

Authors have declared that no competing interests exist.

REFERENCES

1. Olorunfemi MO, Fasuyi SA. Aquifer types and the Geoelectric/Hydrogeologic characteristics of part of the central Basement Terrain of Nigeria (Niger State). *Journal of African Earth Sciences*. 1993; 16:309-317.
2. Ilugbo SO, Adebo BA, Olomo KO, Adebisi AD. Application of Gis and multi criteria decision analysis to geoelectric parameters for modeling of groundwater potential around Ilesha, Southwestern Nigeria. *European Journal of Academic Essays*, 2018;5(5):105-123.
3. Amudu GK, Onwuemesi AG, Ajaegwu NE, Onuba LN, Omali AO. Electrical resistivity investigation for groundwater in the Basement Complex terrain: A case study of Ibadan and its environs, Oyo State, Southwestern Nigeria. *Natural and Applied Sciences Journal*. 2008;9(2):1-12.
4. Amadi AN, Olasehinde PI. Application of Remote Sensing Techniques in Hydrogeological Mapping of parts of Bosso Area, Minna, North Central Nigeria. *International Journal of the Physical Sciences*. 2010;(5):1465-1474.
5. Ilugbo SO, Adebisi AD. Intersection of Lineaments for groundwater prospect analysis using satellite remotely sensed and aeromagnetic dataset around Ibadan, Southwestern Nigeria. *Int. J. of Phys Sci*. 2017;12(23):329-353.
6. Ayodele OS, Odeyemi IB. Analysis of the lineaments extracted from Barker R, LANDSAT TM Image of the Area around Okemesi, South-Western Nigeria. *Indian Journal of Science and Technology*. 2010;3:31-36.
7. Olorunfemi MO, Olarewaju VO, Alade O. On the electrical anisotropy and Ground water yield in a Basement complex area of S.W. Nigeria. *J. Afr. Earth Sci*. 1991; 12(3):462-472.
8. Olorunfemi MO. Voyage on the skin of the earth: A geophysical experience. Inaugural Lecture Series 211, Obafemi Awolowo University, Ile-Ife. 2007;1-2.
9. Billings MP. *Structural Geology* (3rd Edition) 33-34 Prentice-Hall Englewood Cliffs. N.J.; 1972.

10. Maliek SB, Bhattacharya DC, Nag SK. Behavior of fractures in hard rock's: Astudy by surface geology and radial VES methods. *Geoexploration*. 1973;21:529-556.
11. Osun State Ministry of Lands and Physical Planning, Topographical Map of Ilesha south western Sheet. 1965; 234.
12. Vander Velpen BPA. RESIST Version 1.0. M.Sc. Research Project, ITC, Delft Netherland; 2004.
13. Olade MA. General features of a Precambrian iron deposit and its environment at Itakpe Ridge Okene, Nigeria. *Trans. Inst. Min. Metallurgy. Sect.* 1978;B87:81-89.
14. Osun State Ministry of Lands and Physical Planning. Geological Map of Ilesha Iwo Sheet. 1980;60.
15. Rahaman MA. Recent advances in the study of the basement complex of Nigeria. In P. O. Oluyide (Co-ordinator), *Precambrian Geology of Nigeria*. Geol. Surv. Nigeria. Publ. 1988;11-43.
16. KUNETZ G. Principles of direct current prospecting. *Geophys. Monogr.* 1966; 1(1):103.
17. Barker R. Blunk I, Smith I. Geophysical consideration in the design of U.K.National Resistivity Sounding database. *First Break*. 1996;14(2):45-53.
18. Ghosh DP. The application of linear filter theory to the direct interpretation of geoelectrical resistivity sounding measurements. *Geophys. Prospecting*. 1971;19:192-217.

© 2018 Olubusola et al.; This is an Open Access article distributed under the terms of the Creative Commons Attribution License (<http://creativecommons.org/licenses/by/4.0>), which permits unrestricted use, distribution, and reproduction in any medium, provided the original work is properly cited.

Peer-review history:
The peer review history for this paper can be accessed here:
<http://www.sciencedomain.org/review-history/25087>